Evaporation in Hydrological Models Under Rising CO2: A Jump into The Unknown

Thibault Lemaitre-Basset (thibault.lemaitre@inrae.fr)
Sorbonne Université Campus Pierre et Marie Curie: Sorbonne Universite Campus Pierre et Marie Curie
https://orcid.org/0000-0001-6557-429X
Ludovic OUDIN
Sorbonne Université Campus Pierre et Marie Curie: Sorbonne Universite Campus Pierre et Marie Curie
Guillaume THIREL
INRAE Centre Île-de-France Jouy-en-Josas Antony: Institut National de Recherche pour l'Agriculture l'Alimentation et l'Environnement Centre Ile-de-France Jouy-en-Josas Antony

Research Article

Keywords: Potential evaporation, climate projections, runoff projections, CO2 effect

Posted Date: November 30th, 2021

DOI: https://doi.org/10.21203/rs.3.rs-1053044/v1

Evaporation in Hydrological Models Under Rising CO_2: A Jump into The Unknown

Thibault Lemaitre-Basset[1,2], Ludovic Oudin[1], and Guillaume Thirel[2]

[1]Sorbonne Université, CNRS, EPHE, UMR 7619 METIS, Case 105, 4 place Jussieu, F-75005 Paris, France

[2]Université Paris-Saclay, INRAE, HYCAR research unit, Hydrology Research Group, Antony, France

Corresponding author: Thibault Lemaitre-Basset (thibault.lemaitre@inrae.fr)

ABSTRACT

Many hydrological models use the concept of potential evaporation (PE) to simulate actual evaporation. PE formulations often neglect the effect of carbon dioxide (CO_2), which challenges their relevance in a context of climate change and rapid changes in CO_2 atmospheric concentrations. In this work, we implement three options from the literature to take into account the effect of CO_2 on stomatal resistance in the well-known Penman–Monteith PE formulation. We assess their impact on future runoff using the Budyko framework over France. On the basis of an ensemble of Euro-Cordex climate projections using the RCP 4.5 and RCP 8.5 scenarios, we show that taking into account CO_2 in PE formulations largely reduces PE values but also limits projections of runoff decrease, especially under an emissive scenario, namely, the RCP 8.5. Whereas the classic Penman–Monteith formulation yields decreasing runoff projections over most of France, taking into account CO_2 yields more contrasting results. Runoff increase becomes likely in the north of France, which is an energy-limited area, with different levels of runoff response produced by the three tested formulations. The results highlight the sensitivity of hydrological projections to the processes represented in the PE formulation.

Keywords:

Potential evaporation; climate projections; runoff projections; CO_2 effect

Key Points:

We used three options for taking into account CO_2 in the Penman–Monteith potential evaporation formulation.

Potential evaporation is decreased when using CO_2 in the formulation but this decrease depends on how CO_2 is used in the formulation.

In energy-limited areas, future simulated runoff shows higher values when CO_2 is used.

Acknowledgments

The authors acknowledge Météo-France for preparing the EURO-CORDEX climate projections. The first author was funded by Sorbonne University and by Agence de l'Eau Rhin-Meuse.

Funding

The Agence de l'Eau Rhin-Meuse contribute to funds this publication, grant no. AID-2020-00972.

Availability of data and materials

The PE formulation codes used to account for the effect of CO2 on stomatal resistance can be retrieved from: https://doi.org/10.15454/NCNCHG

Author contributions

TLB, LO, and GT conceived the experimental set up and performed the calculation. All authors contributed to the final version of the manuscript.

Declarations

Competing interests

Authors declare have no competing Interests and any financial interest.

Ethics approval

Not applicable.

Consent to participate

Not applicable.

Consent to publish

Not applicable.

1. INTRODUCTION

1.1. Surface–atmosphere interactions in hydrological models

Hydrological models are widely used to assess the regional impacts of climate change on the components of the hydrological cycle (Roudier et al. 2016; Hakala et al. 2019). Most of these hydrological models use conceptual offline (i.e., uncoupled) representations of the soil–vegetation–atmosphere dynamics, through the concept of potential evaporation. The term "evaporation" incorporates two different fluxes: water evaporation from open water surfaces (abiotic process) and plant transpiration resulting from photosynthesis activity (biotic process). Climate change affects evaporation due to increases in air temperature, radiation, and the maximum amount of water vapor in the air. Hereafter, we will focus on the role of carbon dioxide (CO_2) in the representation of the evaporation process for hydrological simulation.

The use of potential evaporation (PE) as an estimation of the atmospheric evaporative demand implicitly assumes rather stationary environmental conditions, e.g., in terms of land use and plant physiology, which is questionable in the current evolving climate and vegetation conditions. Such an assumption might become even more problematic when assessing the water cycle under future changing conditions, which will present drastic modifications in climate and land use. Differences between projected future evaporation rates and water resources obtained from conceptual hydrological models and from more integrative general circulation models were attributed by some authors to the use of a reference PE formulation with fixed parameters (e.g., albedo, constant of the stomatal and aerodynamic resistances, etc.), precluding the possibility of representing changes in vegetation processes (Kumar et al. 2016; Yang et al. 2019). This suggests that the conventional use of "reference" PE needs to be revised in order to improve the realism of hydroclimatic projections (Milly and Dunne 2016).

Adapting the PE formulations is a possible way of taking into account surface–atmosphere interactions in a simplified way. These adaptations include changes in albedo and in stomatal and aerodynamic resistances, which are sensitive to climate and to land use. Among these adaptations, integrating the role of rising atmospheric carbon dioxide (CO_2), in particular, has been investigated in the past decade.

1.2. The role of carbon dioxide in plant water use and how it is parameterized in hydrological models

Plant stomata enable gaseous exchange with the atmosphere for respiration and photosynthesis and they regulate evaporation. It is well-known that under higher atmospheric CO_2 concentrations, the gaseous exchange of plants is altered. The stomatal opening regulates the carbon gain used for photosynthesis and consequently for vegetation growth. Environmental experiments have demonstrated that elevated atmospheric CO_2 concentrations reduce stomatal opening for transpiration in plants (Allen 1990), resulting in a lower water loss through stomata. However, terrestrial vegetation remains an important carbon sink and the feedback from CO_2 fertilization plays a role in PE. An elevated atmospheric CO_2 concentration promotes plant growth and induces a larger leaf surface for evaporation (Le Quéré et al. 2015). It remains under discussion whether the resultant CO_2-induced lower transpiration may be canceled by higher crop transpiration through CO_2-induced increased biomass (Wada et al. 2013). Both effects have been demonstrated and quantified in controlled environments, but transposition of these results under field conditions and over longer time periods is still debated (Rosenberg et al. 1989; Bunce 2004; Cheng et al. 2014). At the global scale, Gedney et al. (2006) found that elevated atmospheric CO_2 concentrations and subsequent stomatal closure were partly responsible for the general upward trend in

111 continental-scale river runoff during the past century, which is confirmed by
112 simulations of several climate models predicting increased runoff in some regions
113 (Yang et al. 2019).

114 Offline impact models such as conceptual hydrological models differ largely in the way
115 they deal with the effects of elevated atmospheric CO_2 concentrations on evaporation.
116 Studies that did not account for CO_2 concentration effects simulated the increase in
117 evaporation due to increased PE as a response to increased air temperature and vapor
118 pressure deficit (Scheff and Frierson 2014; Naumann et al. 2018). This results in a
119 general decrease in soil moisture and river flow, particularly in energy-limited regions
120 (Chiew et al. 2009; Addor et al. 2014; Forzieri et al. 2014; Donnelly et al. 2017).
121 Different results were found in studies where the authors took into account atmospheric
122 CO_2 concentrations (Kruijt et al. 2008; Guillod et al. 2018), suggesting that the
123 inclusion of CO_2 and a more explicit representation of vegetation dynamics can
124 fundamentally change the drought response to climate change (Prudhomme et al. 2014;
125 Pan et al. 2015; Yang et al. 2019).

126 The most straightforward way to take into account elevated CO_2 concentrations in
127 hydrological models is to consider the relationship between changes in CO_2
128 concentrations and changes in stomatal resistance with the Penman–Monteith PE
129 formulation. Based on experimental results, several equations were proposed and
130 applied in impact studies (Allen 1990; Stockle et al. 1992; Yang et al. 2019) but few
131 guidelines exist on the choice of the relationship and its consequences on modeling
132 results.

133

1.3. Scope of the study

This study aims at quantifying the difference between several existing schemes to account for elevated atmospheric CO_2 concentrations in PE estimations and subsequent runoff estimations. On the basis of previous findings, we consider in our analysis only the impact of CO_2 concentrations on stomatal resistance, by applying three existing equations based on the modification of the stomatal resistance r_s in the Penman–Monteith formulation. This study could help to improve PE representation in rainfall–runoff models for climate impact studies and to better quantify corresponding uncertainties. We perform this analysis on the French metropolitan territory, which encompasses both water-limited (in the southern part) and energy-limited (in the northern part) regions, thus potentially showing a contrasting effect of PE estimates on runoff estimation.

2. MATERIALS AND METHODS

2.1. Climate model projections

As the effect of increased CO_2 concentration on stomatal resistance is still limited under 330 ppm, working on past observations does not make it possible to decipher the effect of CO_2 on PE amounts. Consequently, we chose to work on future climate conditions using the outputs of eight CMIP5 general circulation model (GCM)/regional climate model (RCM) couples from EURO-CORDEX (Jacob et al. 2014) under two emission scenarios (Representative Concentration Pathways, RCP4.5 and RCP8.5, see Table 1). A 30-year reference period in the past was selected, from 1970 to 1999, to compute anomalies and the prospective period covers the entire twenty-first century. We used daily outputs of downwelling solar radiation, 2-m air temperature, 10-m wind speed,

158 precipitation, and relative humidity. All the outputs from the eight models were
159 projected on a common regular grid over France with an 8-km spatial resolution,
160 corresponding to the finest resolution of the RCMs. The use of two RCP scenarios
161 makes it possible to assess the sensitivity of the results to the range of elevated
162 atmospheric CO_2 concentration.

163 The evolution of CO_2 concentrations in atmospheric forcing CMIP5 projections is
164 available online: http://www.pik-potsdam.de/~mmalte/rcps/ (Meinshausen et al. 2011).
165 These projections report an increase of 185 ppm and 582 ppm, respectively, for RCP
166 4.5 and RCP 8.5, between 1991 and 2100.

167

168 Table 1: The eight CMIP5 GCM/RCM couples used in this study

General Circulation Model (GCM)	Regional Climate Model (RCM)
CNRM-CM5	CNRM-ALADIN63
CNRM-CM5	KNMI-RACMO22E
IPSL-CM5A-MR	SMHI-RCA4
MOHC-HadGEM2-ES	CLMcom-CCLM4-8-17
ICHEC-EC-EARTH	SMHI-RCA4
MPI-ESM-LR	CLMcom-CCLM4-8-17
MPI-ESM-LR	MPI-CSC-REMO2009
NCC-NorESM1-M	DMI-HIRHAM5

169

170 **2.2. Penman–Monteith PE formulation**

171 We used the FAO56-PM equation (Allen et al. 1998):

172 $$\lambda \cdot PE = \frac{\Delta R_n + (\rho_a \cdot \frac{C_P}{r_a})(e_s - e_a)}{\Delta + \gamma(1 + \frac{r_s}{r_a})}$$

173 where Δ is the slope of saturation vapor pressure versus the air temperature curve
174 (kPa.°C^{-1}), γ is the psychrometric constant (kPa.°C^{-1}), ρ_a is the air density (kg.m^{-3}), C_P
175 is the specific heat of air at constant pressure (J kg^{-1}.°C^{-1}), e_s is the saturation vapor

pressure (kPa) estimated from air temperature (°C) using the equation of Allen et al. (1998), e_a is the actual vapor pressure (kPa) derived from e_s (kPa) and relative humidity (in %), and λ is the latent heat of vaporization (J.kg^{-1}) taken as a constant. Since not all GCM/RCM projections provided net radiation R_n (MJ.m^{-2}.d^{-1}) but instead downwelling short-wave and long-wave solar radiation, net radiation was computed following the recommendations by Allen et al. (1998), using an albedo equal to 0.23 (-) and an upwelling longwave radiation as a function of emissivity and air temperature.

Assuming a grass reference surface of 0.12-m height, Allen et al. (1998) suggested an aerodynamic resistance r_a (s.m^{-1}) inversely proportional to wind speed u (m.s^{-1}) and a constant stomatal resistance r_s (s.m^{-1}):

$$r_a = \frac{208}{u}$$

$$r_s = 70$$

2.3. Adjusting stomatal resistance with atmospheric CO_2 concentrations

From compiling mostly experimental results, several authors proposed adjusting the stomatal resistance with respect to changes in atmospheric CO_2 concentrations. Allen (1990) proposed empirical adjustments of r_s for soybean, sweet corn, and sweetgum based on the experiments by Rogers et al. (1983). Stockle et al. (1992) suggested adjustments of r_s for different types of crops based on the experiments by Morison (1987). Kruijt et al. (2008) compiled several experimental studies to derive r_s adjustments for grass, wood crops, and C4 crops. From a different perspective, Yang et al. (2019) proposed a relationship between the change in r_s and the change in atmospheric CO_2 concentrations, so that the estimated evaporation from the Choudhury

model fits the estimated evaporation simulated by several CMIP5 models under the RCP 8.5 scenario.

These proposed adaptations of r_s were all expressed as a fraction of a reference stomatal resistance r_{s_ref} at the atmospheric concentration of CO_2 equal to 330 ppm. The resulting functional relationships between stomatal resistance and atmospheric CO_2 are shown in Figure 1.

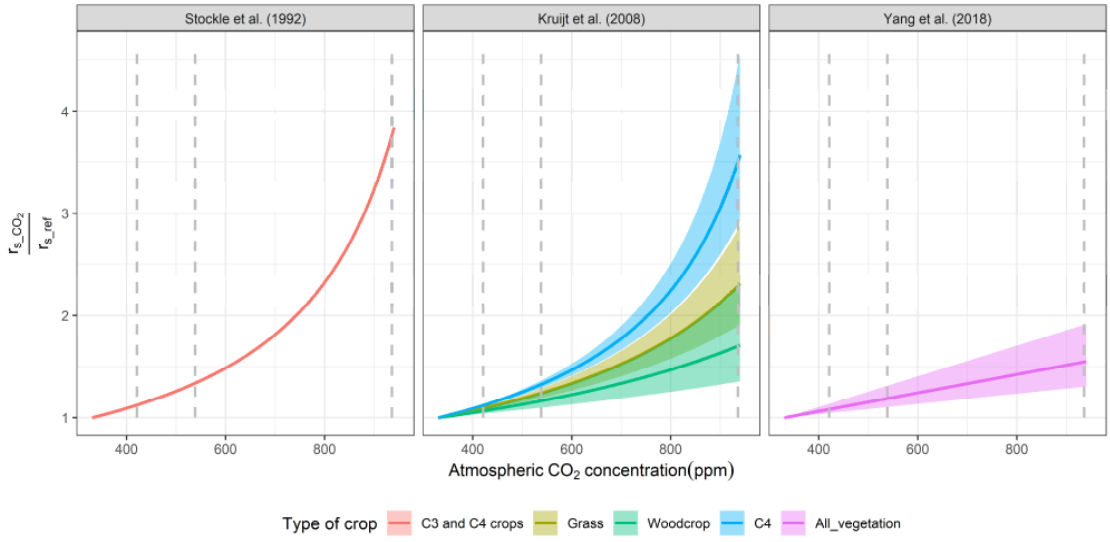

Fig. 1 Functional relationships between relative change in r_s and atmospheric CO_2 concentration. Uncertainty bounds are computed using the information from the original publications. Since Yang et al. (2019) did not explicitly take into consideration plant species, we retained the adaptations obtained from the mean climate model simulations and for the individual climate models representing the lower and upper bounds. The dashed vertical lines refer to the expected atmospheric CO_2 concentrations for 2100 under RCP 2.6 (left line), RCP 4.5 (middle line), and RCP 8.5 (right line).

In this paper, we did not consider the effect of plant species on r_s, and to remain consistent with PE usage in hydrological models, we retained only the equation proposed by Kruijt et al. (2008) corresponding to grass. Consequently, three functional relationships between relative change in r_s and atmospheric CO_2 concentration were used. The selection was made based on actual usage of these relationships for hydrological model applications. Table 2 presents the selected relationships, their acknowledged limits, and an inexhaustive list of some applications for hydrological modeling.

Table 2: Functional relationships used in this study to assess the impact of CO_2. $r_{s\_Stockle}$ r_{s_Kruijt} and r_{s_Yang}refer to the modified stomatal resistances taking into account elevated atmospheric CO_2, r_{s_ref} is the reference stomatal resistance taken in this study at 70 s.m^{-1}, and $CO_{2_{ref}}$ is the reference concentration of atmospheric CO_2, taken at 330 ppm in this study.

Original reference	Notation	Equation used in this study	Comments	Previous hydrological applications
Stockle et al. (1992)	r_{s_Stockle}	$\frac{r_{s\_\mathrm{Stockle}}}{r_{s\_ref}} = \frac{1}{1.4 - 0.4\frac{\mathrm{CO_2}}{\mathrm{CO_{2_{ref}}}}}$	Derived from experimental results for C3 and C4 crops. The range of applicability is up to 660 ppm.	Mainly SWAT model applications (Wu et al. 2012; Butcher et al. 2014; Kim et al. 2017)
Kruijt et al. (2008)	r_{s_Kruijt}	$\frac{r_{s\_\mathrm{Kruijt}}}{r_{s\_ref}} = \frac{1}{1 - 9.3 \cdot 10^{-4}\left(\mathrm{CO_2} - \mathrm{CO_{2_{ref}}}\right)}$	Derived from experimental results for three types of crops, the equation used here is for grass. The range of applicability is up to 660 ppm.	Some national case studies with diverse rainfall–runoff models (Kruijt et al. 2008; Rasmussen et al. 2012; Rudd and Kay 2015; Guillod et al. 2018)
Yang et al. (2018)	r_{s_Yang}	$\frac{r_{s\_\mathrm{Yang}}}{r_{s\_ref}} = 1 + 9 \cdot 10^{-4}\left(\mathrm{CO_2} - \mathrm{CO_{2_{ref}}}\right)$	Derived by fitting the evaporation simulated by the Choudhury model to the evaporation simulated by climate model.	(Yang et al. 2019)

2.4. Budyko model

A change in PE does not necessarily lead to similar changes in runoff, due to the additional influence of soil moisture (Duethmann and Blöschl 2018). To account for these additional influences, we analyzed the evolution of annual runoff (Q) using the non-parametric Budyko (1974) equation:

$$Q = P - P\left[\frac{PE}{P} \cdot \tanh\left(\frac{P}{PE}\right) \cdot \left(1 - e^{-\frac{PE}{P}}\right)\right]^{\frac{1}{2}}$$

with *P* the precipitation and all variables expressed in mm.y^{-1}. The Budyko equation is one of the most widely used approaches to determine long-term evaporation. This equation is derived from long-term climate observations and highlights the connection

of evaporation with both precipitation and PE. With climate projections of both P and PE, this approach makes it possible to investigate the potential change in runoff under several climate projections. Thus, the Budyko framework has been used in climate impact studies at the national scale (Donohue et al. 2011; Renner and Bernhofer 2012; van der Velde et al. 2014). In this study, the Budyko equation is applied at the annual time scale, for each 8×8-km cell of the regular grid over France. This approach allows us to assess both (a) the temporal evolution of P, PE, and runoff over the entire domain and (b) the regional differences in these evolutions. Since RCM climate outputs may be biased, all results are shown as anomalies with respect to the 1970–1999 period, taken as the reference.

3. RESULTS

3.1. Changes in climate inputs and Budyko runoff depending on the PE CO_2 parametrization

Precipitation anomalies are shown in Figure 2 since they influence the simulated runoff in the Budyko equation. Precipitation trends are highly variable among RCMs, showing on average no trend under RCP 4.5 in the future relative to the reference period 1970–1999, and a slight decreasing trend by the end of the century under RCP 8.5 ($\Delta P = -22$ mm.y^{-1}, corresponding to a relative decrease of –2 %).

The impact of the choice of stomatal resistance on PE is evident for both RCP 4.5 and RCP 8.5 scenarios (Figure 2). For RCP 4.5, the ensemble of climate models projects an increasing PE in the future relative to the reference period 1970–1999. All formulations that increase r_s with rising CO_2 lead to a lower PE increase compared to the reference Penman–Monteith formulation. The largest increase ($\Delta PE = +78$ mm.y^{-1} by the end of

the century, corresponding to a relative increase of +11%) is obtained with the Penman–Monteith equation applied with constant r_s. Conversely, $r_{s\_Stockle}$ leads to a moderate increase (ΔPE is +33 mm.y^{-1} by the end of the century, corresponding to a relative increase of +5%). For RCP 8.5, the evolutions in PE anomalies diverge and the trends depend greatly on the formulation of r_s chosen. The Penman–Monteith equation applied with constant r_s leads again to a more pronounced increase (ΔPE = +149 mm.y^{-1}, corresponding to a relative increase of +21%). Conversely, the Penman–Monteith equation with modified $r_{s\_Stockle}$ leads to a decreasing PE at the end of the century (ΔPE = –20 mm.y^{-1}, corresponding to a relative change of –3%), after a period of moderate increase until the 2070s. The two other formulations of r_s tested yield intermediate positive changes. The increase in PE is more pronounced from RCP 4.5 to RCP 8.5 using r_{s_Yang}, while r_{s_Kruijt} yields a lower increase under the RCP 8.5 scenario, showing that the increase in PE due to enhanced vapor pressure deficit is offset by the increase in stomatal resistance due to rising CO_2. The PE uncertainties due to RCM projections generally increase during the period. Under the RCP 4.5 scenario, the uncertainties in PE due to climate projections are comparable to the uncertainties in PE due to the r_s formulation, while PE uncertainties due to the r_s formulation are larger under RCP 8.5.

The implications of these different PE evolutions for simulated runoff are evident although dependent also on precipitation evolution (Figure 2). For the RCP 4.5 scenario, the ensemble of climate models projects a limited decrease in simulated runoff in the future relative to the reference period 1970–1999 (ΔQ ranges from –40 mm.y^{-1} to –14 mm.y^{-1} by the end of the century, corresponding to relative changes of –6% to –2%, respectively). For the RCP 8.5 scenario, runoff anomaly evolutions are globally negative but diverge more among PE formulations. The Penman–Monteith equation applied with constant r_s leads to the most pronounced decrease (ΔQ = –99 mm.y^{-1} by

the end of the century, corresponding to a relative decrease of –14%), while Penman–Monteith $r_{s\_Stockle}$ leads to a very slight decrease (ΔQ = –4 mm.y^{-1}, corresponding to a relative change of –1%). There is a large variability among climate model simulations and some climate models project positive runoff changes for both RCP 4.5 and RCP 8.5, whatever the r_s formulation used.

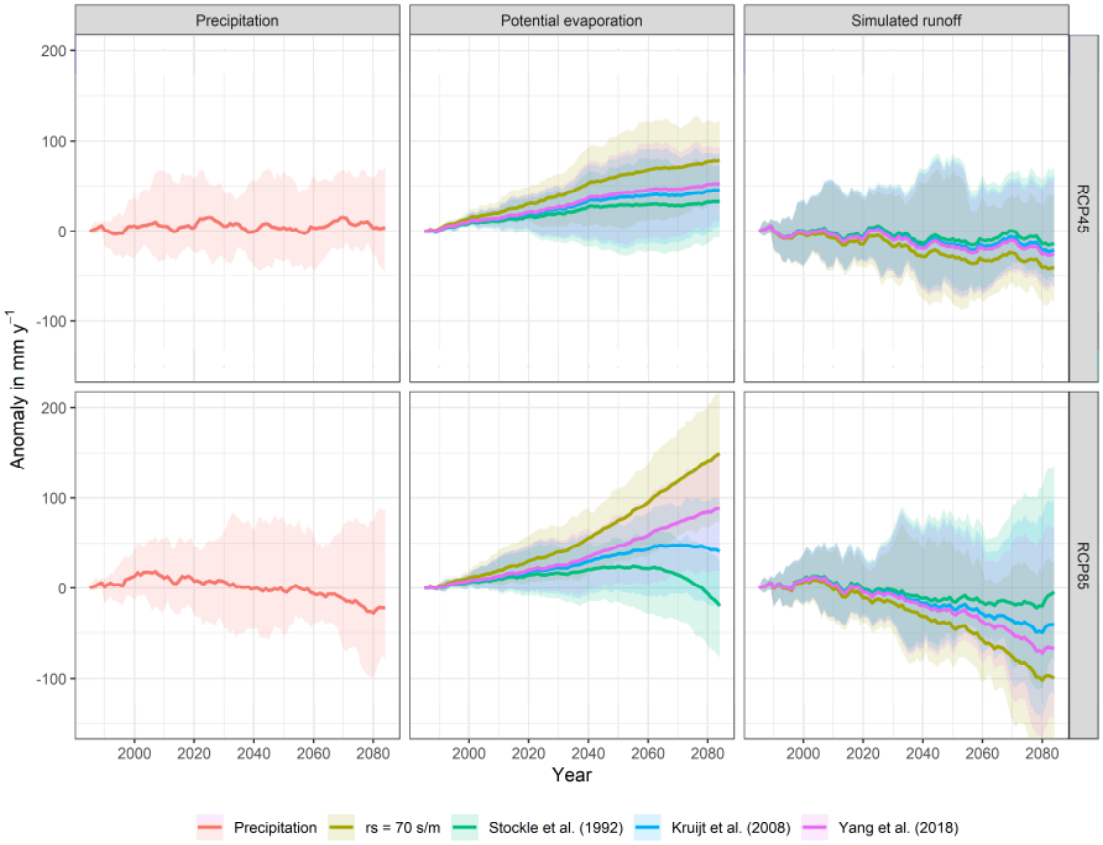

Fig. 2 Evolution of precipitation (left), PE (middle), and simulated runoff using the Budyko equation (right) relative to the 1970–1999 period for the RCP 4.5 and RCP 8.5 scenarios, averaged over France. The colored shadings represent the min–max estimation range from to climate models and the solid lines represent the mean. Data are smoothed with a 30-year running mean. Detailed values are given in Appendix A.

3.2. Spatial patterns of changes

There is a meridional gradient for precipitation changes over France, with negative and positive trends in the southern and northern parts, respectively (Figure 3). This gradient is more important for RCP 8.5 than for RCP 4.5. The magnitude of differences between the selected adaptations of stomatal resistance is in agreement with the time series

presented in Figure 2. Under RCP 8.5, r_{s_Stockle} and r_{s_Kruijt} formulations produce a decreasing PE (up to –15%) in some regions, particularly over the northwestern coast. For these regions, positive trends in precipitation and negative trends in PE suggest larger spatial discrepancies in the simulated runoff. For RCP 4.5, for the reference formulation and r_{s_Yang}, an increase in PE is projected over the whole territory.

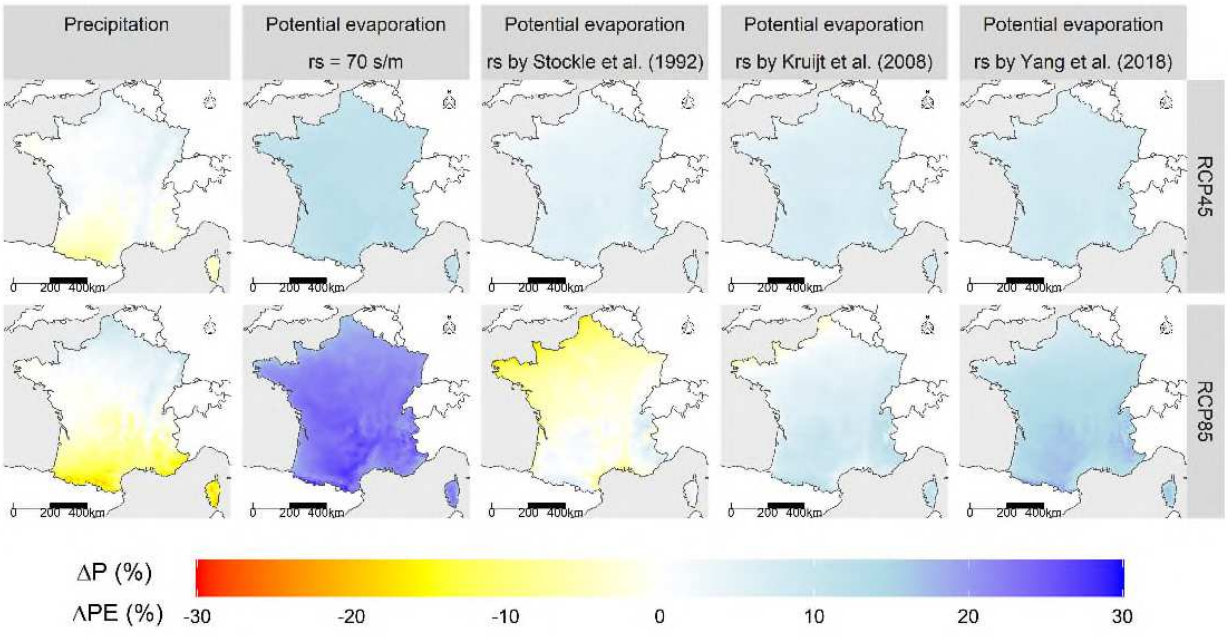

Fig. 3 Ensemble mean of relative annual precipitation and PE changes (%) between the 1970–1999 and 2070–2099 periods under the RCP 4.5 and RCP 8.5 scenarios with different formulations of stomatal resistance.

Spatial patterns of simulated runoff changes vary dramatically across the selected formulations of stomatal resistance (Figure 4). The decrease is general using the Penman–Monteith equation applied with constant r_s, with southern regions experiencing a decrease that can reach –50%. The adaptations of the stomatal resistance provide a more nuanced picture, with a decrease in runoff in southern areas and an increase in runoff in the northern areas, up to +30 %. These uncertainties in the sign of runoff changes are also evident across climate projections, since climate model trends agree only in limited areas, whatever the PE formulation selected (Figure 5). Only for

RCP 8.5 and southern France is there agreement between the eight models on a decreased runoff.

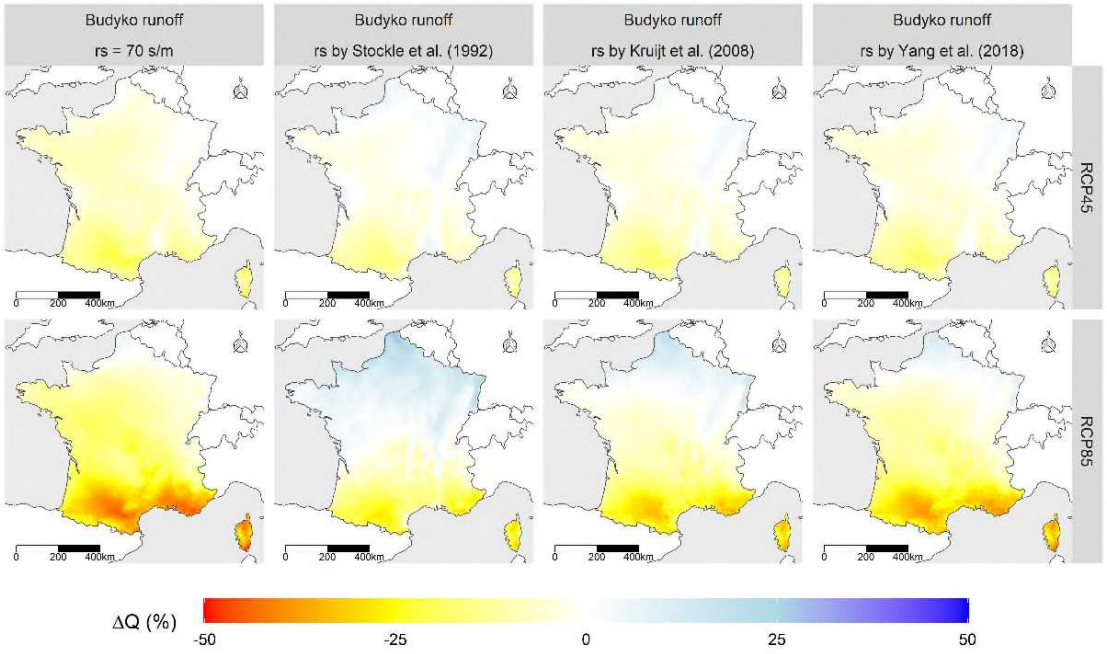

Fig. 4 Ensemble mean of relative annual simulated runoff changes (%) using the Budyko equation between the 1970–1999 and 2070–2099 periods under the RCP 4.5 and RCP 8.5 scenarios with different formulations of stomatal resistance.

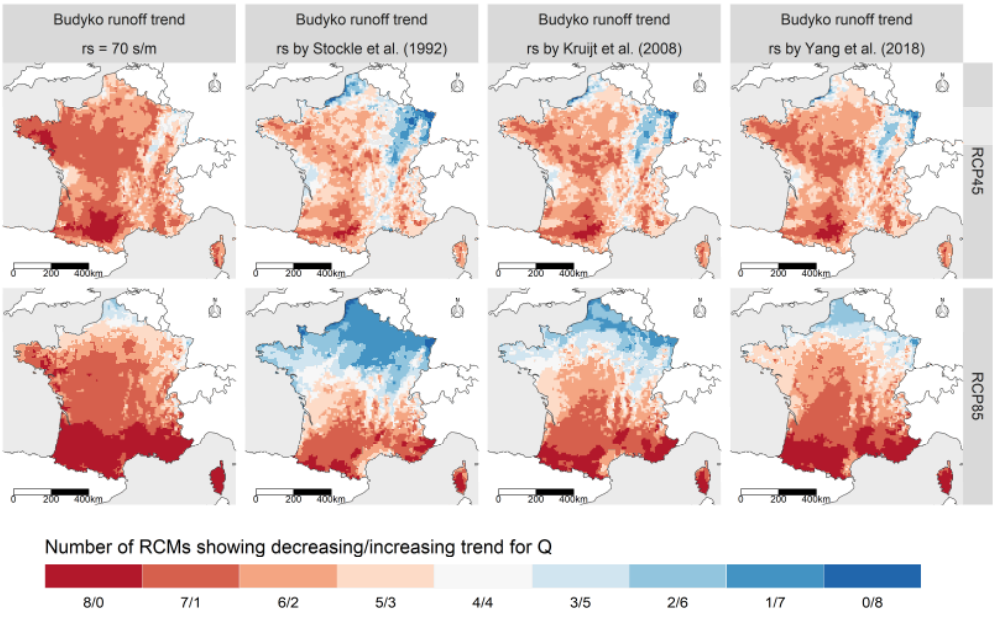

Fig. 5 Partition of the number of RCMs (out of 8) showing decreasing / increasing runoff using the Budyko equation between the 1970–1999 and 2070–2099 periods under the RCP 4.5 and RCP 8.5 scenarios with different formulations of stomatal resistance.

3.3. Comparison with runoff as estimated by RCMs

The runoff averaged over France as simulated by RCMs (taken as precipitation minus evaporation) presents relatively similar trends to those obtained with the Budyko equation (Figure 6). For the RCP 4.5 scenario, the runoff decreases slightly over time, in general agreement with the runoff estimated under the Budyko framework with the different PE formulations. For the RCP 8.5 scenario, runoff anomalies from RCMs are globally negative (except for Stockle's formulation) but less pronounced than those estimated under the Budyko framework. The mean of the RCM ensemble leads to a very slight decrease (ΔQ = -31 mm.y^{-1}), a value that lies between the runoff simulated with r_{s_Kruijt} (ΔQ = –40 mm.y^{-1}) and the one obtained with r_{s_Stockle} (ΔQ = –4 mm.y^{-1}). The simulated runoff from the Penman–Monteith equation applied with constant r_s leads to a clearly more important decrease that is close to the minimum of the runoff estimates.

The spatial patterns of changes in runoff (Figure 6) corroborate these findings: For both RCP 4.5 and RCP 8.5, the spatial patterns of change given by the RCMs are close to those obtained using r_{s_Stockle} and r_{s_Kruijt}, i.e., a distinct trend between northern and southern regions.

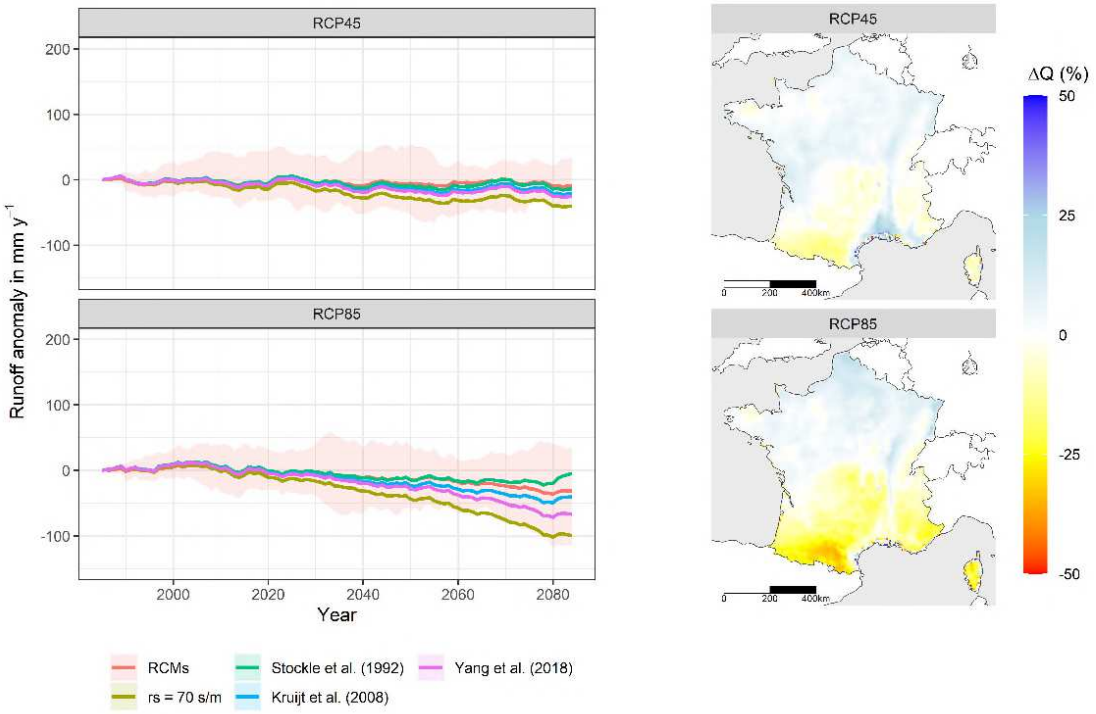

345

346 **Fig. 6** Left: Evolution of simulated runoff using the RCM simulations relative to the 1970–1999 period for the RCP
347 4.5 and RCP 8.5 scenarios. The colored shadings represent the min-max estimation range in RCMs runoff estimation
348 and the solid lines represent the mean. Data are smoothed with a 30-year running mean. Right: Ensemble mean of
349 relative annual RCMs simulated runoff changes (%) between the 1970–1999 and 2070–2099 periods under the RCP
350 4.5 and RCP 8.5 scenarios.

351

352 ## 4. DISCUSSION

353 ### 4.1. Comparing changes with previous model experiments

354 The Budyko equation used in this study to simulate runoff is relatively
355 straightforward and neglects key processes such as the seasonality of P and PE. Besides,
356 the climate projections from RCMs used in this paper were not bias-corrected. Thus,
357 we did not intend to produce reliable estimates of the impact of climate, but rather to
358 investigate the spectrum of changes associated with the choice of a formulation of PE
359 that takes into account the influence of CO_2 on stomatal resistance. The regional pattern
360 changes in annual runoff obtained in this study are, however, in agreement with
361 previous studies (Donnelly et al. 2017; Dayon et al. 2018) that used more complex
362 hydrological models: a pronounced decline in mean streamflow in the southern part of

363 France, no clear streamflow changes in the northern part of France, with large
364 uncertainties stemming from climate projections. We also showed that these patterns
365 are in general agreement with RCM outputs, which means that despite the simplicity of
366 the Budyko equation, it enables us to reproduce the simulation of more physically based
367 coupled climate models.

368

369 **4.2. Perspectives of using r_s formulations accounting for CO_2 in PE**
370 **formulations in future studies**

371 As expected, taking into account the influence of CO_2 on r_s limits evaporation
372 and thus also limits the decline in runoff, particularly in energy-limited regions. The
373 choice of the formulation of r_s is therefore all but insignificant for studies on the impact
374 of climate change. The three formulations tested in this paper provide quite different
375 runoff projections compared with the classic use of the Penman–Monteith equation with
376 constant r_s. The differences are obvious under the RCP 8.5 but also present under the
377 RCP 4.5 scenario. It is noteworthy that the different trends (and sign of the trend) are
378 highly variable compared to differences of changes in PE when considering different
379 PE formulations (Lemaitre-Basset et al. 2021), showing that the uncertainties in
380 projections of CO_2 concentrations might be translated to large uncertainties in PE (and
381 simulated runoff).

382 While the use of the Budyko framework highlights moderate-to-important impacts of
383 taking into account CO_2 in PE formulations, how this could reflect on hydrological
384 projections made with rainfall–runoff hydrological models might not be
385 straightforward. The impact of PE formulations on discharge projections is still under
386 debate, some studies pointing to either a low impact (Dakhlaoui et al. 2020) or a high

impact (Seiller and Anctil 2016). Specifically, the presence of a parameter calibration in most hydrological models might distort the relationship between PE anomalies and runoff anomalies (Oudin et al. 2006) and could lead to different results from those simulated with the Budyko framework.

4.3. Limitations of taking into account CO_2 in PE formulations

While there are many good reasons for adjusting r_s with CO_2, the choice of a single formulation is complicated. Two existing formulations, namely, the formulations by Stockle et al. (1992) and by Kruijt et al. (2008), were developed from experimental results for selected types of crops, and their range of applicability is up to 660 ppm, i.e., far below the expected CO_2 content by the end of century under the RCP 8.5 scenario (935 ppm in 2100). Indeed, increasing stomatal resistance indefinitely is not realistic, as plants must continue to ensure gas exchange, even with a highly enriched CO_2 atmosphere. Thus, the use of these empirical formulations for the RCP 8.5 scenario is as questionable as the use of these formulations for large-scale applications with mixed land use. The third formulation, proposed by Yang et al. (2019), was derived by fitting the evaporation simulated by the Choudhury model to the evaporation simulated by climate models, the rationale being that climate models allow us to take into account surface–atmosphere interactions more explicitly. This formulation was calibrated at the global scale and we showed that it probably needs some regional adjustments, since the runoff simulated using this formulation is not fully in line with RCM outputs over France.

The fertilization effect of atmospheric CO_2 on the growth of plants may produce an opposite effect by promoting evaporation. Nevertheless, this theory is in fact limited

411 in the context of long-term exposure (climate change): Ainsworth and Rogers (2007)
412 showed a reduction in photosynthesis activity, called "down-regulation." Besides, plant
413 growth needs fertilizers (e.g., nitrogen), and their availability in the environment will
414 limit the fertilization effect of CO_2, thus reducing the CO_2 sink role of terrestrial
415 vegetation (Wang et al. 2020). This competing effect of CO_2 on evaporation can
416 theoretically be taken into account in r_s formulations through the use of the leaf area
417 index (LAI). However, determining LAI in the future requires a dynamic vegetation
418 model and presents relatively high uncertainties (Yang et al. 2019). Over France,
419 simulated LAI with different GCMs generally shows a positive trend (between 0.05
420 $\%.y^{-1}$ in the south and 0.1 $\%.y^{-1}$ in the north). Since the formulation proposed by Yang
421 et al. (2019) was derived by minimizing the discrepancies between evaporation
422 simulated by Budyko and GCMs, it implicitly takes into account the positive role of
423 LAI. This may explain the lower effect of CO_2 on stomatal resistance compared with
424 Stockle et al. (1992) and Kruijt et al. (2008).

425 The use of simple functional relationships between r_s and CO_2 for correcting PE
426 estimates may be seen as "flogging a dead horse." Translating complex surface–
427 atmosphere feedbacks into a simple adjustment of the PE equation neglects several
428 other possible effects. For example, Xiao et al. (2020) showed that actual evaporation
429 tends to decline under climate change, owing to decreased relative humidity and
430 consequent stomatal closure due to the decreased moisture gradient at the leaf surface.
431 Nevertheless, for most PE formulations, the opposite occurred, since reducing relative
432 humidity increases PE.

433

5. CONCLUSION

In this study, we assessed the impact of taking into account CO_2 in the Penman–Monteith PE formulation. We showed that taking into account CO_2 in this PE formulation leads to reduced PE amounts. On the basis of the Budyko framework, we have shown that the inclusion of CO_2 in PE formulations limits the annual runoff reduction, especially in an emissive scenario, namely, the RCP 8.5 scenario, and even increases annual runoff in some regions. Whereas the classic Penman–Monteith formulation leads to decreasing runoff projections over most of France, taking into account CO_2 leads to more contrasting results, with runoff increase that becomes likely in the north of France, which is an energy-limited area. However, the three formulations tested involve different shades of runoff response. The results suggest that climate change impact studies that use PE formulations that do not make use of CO_2 may underestimate runoff under a future climate. However, uncertainty remains in the way CO_2 can be included in PE formulations, as can be seen from the three options tested here, which questions the intensity of hydrological projection changes due to the inclusion of CO_2.

The common way to compute PE for hydrological models in climate impact studies ignores the negative feedback from terrestrial vegetation on evaporation. To correct the bias between PE evolution and actual evaporation in climate impact studies, we recommend estimating PE with an adjusted Penman–Monteith formulation, or another form (e.g., Peiris and Döll, 2021). The use of the approach developed by Yang et al. (2019) is probably better suited to both scenarios, unlike the empirical approaches of Stockle et al. (1992) and Kruijt et al. (2008) that are not suited to the high emissive scenarios. Finally, further observations are needed to include the effect of vegetation feedback on PE more precisely: including the evolution of vegetation yield through,

459 e.g., simulated evolution of leaf area index, and limitation of the air vapor–pressure
460 deficit on evaporation.

Appendix A: Detailed P, PE, and runoff values depending on RCP and formulation of r_s

Table 3: Values of P, PE, and simulated runoff using the Budyko equation for two climate periods (1970–1999 and 2070–2099) depending on the choice of r_s and the RCP. The mean value over the 8 GCMs/RCMs is indicated along with the min–max range.

	Historical	RCP 4.5			RCP 8.5		
Variable	Period (1970–1999) in mm.y^{-1}	Period (2070–2099) in mm.y^{-1}	Anomaly in mm.y^{-1}	Anomaly in percentage	Period (2070–2099) in mm.y^{-1}	Anomaly in mm.y^{-1}	Anomaly in percentage
Precipitation	1191 [811, 1421]	1195 [802, 1459]	4 [–45, 71]	0 [–4, 6]	1169 [762, 1413]	–22 [–78, 87]	–2 [–7, 7]
Potential evaporation with r_{s_ref}	686 [613, 765]	765 [664, 887]	78 [36, 123]	11 [5, 16]	836 [732, 979]	149 [74, 215]	21 [11, 28]
Potential evaporation with r_{s_Stockle}	683 [610, 762]	716 [621, 834]	33 [–6, 73]	5 [–1, 10]	664 [576, 790]	–20 [–77, 29]	–3 [–11, 4]
Potential evaporation with r_{s_Kruijt}	684 [611, 762]	729 [632, 848]	45 [6, 87]	6 [1, 11]	725 [632, 858]	41 [–23, 97]	6 [–3, 13]
Potential evaporation with $r_{s_{\mathrm{Yang}}}$	680 [607, 758]	733 [635, 852]	53 [12, 95]	8 [2, 13]	768 [671, 905]	88 [19, 148]	13 [3, 20]
Simulated runoff with r_{s_ref}	789 [383, 1032]	749 [328, 1002]	–40 [–80, 42]	–6 [–14, 5]	690 [271, 906]	–99 [–180, 30]	–14 [–29, 4]
Simulated runoff with r_{s_Stockle}	791 [384, 1034]	777 [346, 1031]	–14 [–54, 72]	–2 [–10, 9]	786 [331, 1011]	–4 [–79, 136]	–1 [–14, 16]
Simulated runoff with r_{s_Kruijt}	790 [384, 1033]	769 [341, 1023]	–21 [–61, 64]	–3 [–11, 8]	750 [307, 971]	–40 [–118, 97]	–6 [–20, 12]
Simulated runoff with $r_{s_{\mathrm{Yang}}}$	793 [386, 1036]	768 [340, 1021]	–25 [–66, 59]	–4 [–12, 7]	726 [292, 945]	–67 [–147, 68]	–10 [–24, 8]

References

Addor N, Rössler O, Köplin N, et al (2014) Robust changes and sources of uncertainty in the projected hydrological regimes of Swiss catchments. Water Resour Res 50:7541–7562. https://doi.org/10.1002/2014WR015549

Ainsworth EA, Rogers A (2007) The response of photosynthesis and stomatal conductance to rising [CO_2]: mechanisms and environmental interactions: Photosynthesis and stomatal conductance responses to rising [CO_2]. Plant Cell Environ 30:258–270. https://doi.org/10.1111/j.1365-3040.2007.01641.x

Allen LH (1990) Plant Responses to Rising Carbon Dioxide and Potential Interactions with Air Pollutants. J Environ Qual 19:15–34. https://doi.org/10.2134/jeq1990.00472425001900010002x

Allen RG, Pereira L, Raes D, Smith M (1998) Crop evapotranspiration: guidelines for computing crop water requirements. FAO, Rome, Italy

Budyko MI (1974) Climate and Life, English ed édition (David H. Miller, Translator). Geniza, New York

Bunce JA (2004) Carbon dioxide effects on stomatal responses to the environment and water use by crops under field conditions. Oecologia 140:1–10. https://doi.org/10.1007/s00442-003-1401-6

Butcher JB, Johnson TE, Nover D, Sarkar S (2014) Incorporating the effects of increased atmospheric CO_2 in watershed model projections of climate change impacts. J Hydrol 513:322–334. https://doi.org/10.1016/j.jhydrol.2014.03.073

Cheng L, Zhang L, Wang Y-P, et al (2014) Impacts of elevated CO2, climate change and their interactions on water budgets in four different catchments in Australia. J Hydrol 519:1350–1361. https://doi.org/10.1016/j.jhydrol.2014.09.020

Chiew FHS, Teng J, Vaze J, et al (2009) Estimating climate change impact on runoff across southeast Australia: Method, results, and implications of the modeling method. Water Resour Res 45:. https://doi.org/10.1029/2008WR007338

Dakhlaoui H, Seibert J, Hakala K (2020) Sensitivity of discharge projections to potential evapotranspiration estimation in Northern Tunisia. Reg Environ Change 20:34. https://doi.org/10.1007/s10113-020-01615-8

Dayon G, Boé J, Martin E, Gailhard J (2018) Impacts of climate change on the hydrological cycle over France and associated uncertainties. Comptes Rendus Geosci 350:. https://doi.org/10.1016/j.crte.2018.03.001

Donnelly C, Greuell W, Andersson J, et al (2017) Impacts of climate change on European hydrology at 1.5, 2 and 3 degrees mean global warming above preindustrial level. Clim Change 143:13–26. https://doi.org/10.1007/s10584-017-1971-7

503 Donohue RJ, Roderick ML, McVicar TR (2011) Assessing the differences in
504 sensitivities of runoff to changes in climatic conditions across a large basin. J
505 Hydrol 406:234–244. https://doi.org/10.1016/j.jhydrol.2011.07.003

506 Duethmann D, Blöschl G (2018) Why has catchment evaporation increased in the past
507 40 years? A data-based study in Austria. Hydrol Earth Syst Sci 22:5143–5158.
508 https://doi.org/10.5194/hess-22-5143-2018

509 Forzieri G, Feyen L, Rojas R, et al (2014) Ensemble projections of future streamflow
510 droughts in Europe. Hydrol Earth Syst Sci 18:85–108.
511 https://doi.org/10.5194/hess-18-85-2014

512 Gedney N, Cox PM, Betts RA, et al (2006) Detection of a direct carbon dioxide effect
513 in continental river runoff records. Nature 439:835–838.
514 https://doi.org/10.1038/nature04504

515 Guillod BP, Jones RG, Dadson SJ, et al (2018) A large set of potential past, present and
516 future hydro-meteorological time series for the UK. Hydrol Earth Syst Sci
517 22:611–634. https://doi.org/10.5194/hess-22-611-2018

518 Hakala K, Addor N, Teutschbein C, et al (2019) Hydrological Modeling of Climate
519 Change Impacts. In: Encyclopedia of Water. American Cancer Society, pp 1–
520 20

521 Jacob D, Petersen J, Eggert B, et al (2014) EURO-CORDEX: new high-resolution
522 climate change projections for European impact research. Reg Environ Change
523 14:563–578. https://doi.org/10.1007/s10113-013-0499-2

524 Kim Y, Band LE, Ficklin DL (2017) Projected hydrological changes in the North
525 Carolina piedmont using bias-corrected North American Regional Climate
526 Change Assessment Program (NARCCAP) data. J Hydrol Reg Stud 12:273–
527 288. https://doi.org/10.1016/j.ejrh.2017.06.005

528 Kruijt B, Witte J-PM, Jacobs CMJ, Kroon T (2008) Effects of rising atmospheric CO_2
529 on evapotranspiration and soil moisture: A practical approach for the
530 Netherlands. J Hydrol 349:257–267.
531 https://doi.org/10.1016/j.jhydrol.2007.10.052

532 Kumar S, Zwiers F, Dirmeyer PA, et al (2016) Terrestrial contribution to the
533 heterogeneity in hydrological changes under global warming. Water Resour Res
534 52:3127–3142. https://doi.org/10.1002/2016WR018607

535 Le Quéré C, Moriarty R, Andrew RM, et al (2015) Global Carbon Budget 2015. Earth
536 Syst Sci Data 7:349–396. https://doi.org/10.5194/essd-7-349-2015

537 Lemaitre-Basset T, Oudin L, Thirel G, Collet L (2021) Unravelling the contribution of
538 potential evaporation formulation to uncertainty under climate change. Hydrol
539 Earth Syst Sci Discuss 1–18. https://doi.org/10.5194/hess-2021-361

540 Meinshausen M, Smith SJ, Calvin K, et al (2011) The RCP greenhouse gas
541 concentrations and their extensions from 1765 to 2300. Clim Change 109:213–
542 241. https://doi.org/10.1007/s10584-011-0156-z

543 Milly PCD, Dunne KA (2016) Potential evapotranspiration and continental drying. Nat
544 Clim Change 6:946–949. https://doi.org/10.1038/nclimate3046

545 Morison JIL (1987) Intercellular CO2 concentration and stomatal response to CO_2. In:
546 Stomatal function, eds E. Zeiger, G.D.Farquhar & I.R. Cowan. Stanford
547 University Press, Stanford, pp 229–252

548 Naumann G, Alfieri L, Wyser K, et al (2018) Global Changes in Drought Conditions
549 Under Different Levels of Warming. Geophys Res Lett 45:3285–3296.
550 https://doi.org/10.1002/2017GL076521

551 Oudin L, Perrin C, Mathevet T, et al (2006) Impact of biased and randomly corrupted
552 inputs on the efficiency and the parameters of watershed models. J Hydrol
553 320:62–83, https://doi.org/10.1016/j.jhydrol.2005.07.016

554 Pan S, Tian H, Dangal SRS, et al (2015) Responses of global terrestrial
555 evapotranspiration to climate change and increasing atmospheric CO_2 in the 21st
556 century. Earths Future 3:15–35. https://doi.org/10.1002/2014EF000263

557 Peiris TA, Döll P (2021) A simple approach to mimic the effect of active vegetation in
558 hydrological models to better estimate hydrological variables under climate
559 change , EGU General Assembly 2021, online, 19–30 Apr 2021, EGU21-12025,
560 https://doi.org/10.5194/egusphere-egu21-12025

561 Prudhomme C, Giuntoli I, Robinson EL, et al (2014) Hydrological droughts in the 21st
562 century, hotspots and uncertainties from a global multimodel ensemble
563 experiment. Proc Natl Acad Sci 111:3262–3267.
564 https://doi.org/10.1073/pnas.1222473110

565 Rasmussen J, Sonnenborg TO, Stisen S, et al (2012) Climate change effects on
566 irrigation demands and minimum stream discharge: impact of bias-correction
567 method. Hydrol Earth Syst Sci 16:4675–4691. https://doi.org/10.5194/hess-16-
568 4675-2012

569 Renner M, Bernhofer C (2012) Applying simple water-energy balance frameworks to
570 predict the climate sensitivity of streamflow over the continental United States.
571 Hydrol Earth Syst Sci 16:2531–2546. https://doi.org/10.5194/hess-16-2531-
572 2012

573 Rogers HH, Bingham GE, Cure JD, et al (1983) Responses of Selected Plant Species
574 to Elevated Carbon Dioxide in the Field. J Environ Qual 12:569–574.
575 https://doi.org/10.2134/jeq1983.00472425001200040028x

576 Rosenberg NJ, McKenney MS, Martin P (1989) Evapotranspiration in a greenhouse-
577 warmed world: A review and a simulation. Agric For Meteorol 47:303–320.
578 https://doi.org/10.1016/0168-1923(89)90102-0

579 Roudier P, Andersson J, Donnelly C, et al (2016) Projections of future floods and
580 hydrological droughts in Europe under a +2°C global warming. Clim Change
581 135:. https://doi.org/10.1007/s10584-015-1570-4

582 Rudd AC, Kay AL (2015) Use of very high resolution climate model data for
583 hydrological modelling: estimation of potential evaporation. Hydrol Res
584 47:660–670. https://doi.org/10.2166/nh.2015.028

585 Scheff J, Frierson DMW (2014) Scaling Potential Evapotranspiration with Greenhouse
586 Warming. J Clim 27:1539–1558. https://doi.org/10.1175/JCLI-D-13-00233.1

587 Seiller G, Anctil F (2016) How do potential evapotranspiration formulas influence
588 hydrological projections? Hydrol Sci J 61:2249–2266.
589 https://doi.org/10.1080/02626667.2015.1100302

590 Stockle CO, Williams JR, Rosenberg NJ, Jones CA (1992) A method for estimating the
591 direct and climatic effects of rising atmospheric carbon dioxide on growth and
592 yield of crops: Part I--Modification of the EPIC model for climate change
593 analysis. Agric Syst 38:225–238

594 van der Velde Y, Vercauteren N, Jaramillo F, et al (2014) Exploring hydroclimatic
595 change disparity via the Budyko framework. Hydrol Process 28:4110–4118.
596 https://doi.org/10.1002/hyp.9949

597 Wada Y, Wisser D, Eisner S, et al (2013) Multimodel projections and uncertainties of
598 irrigation water demand under climate change. Geophys Res Lett 40:4626–
599 4632. https://doi.org/10.1002/grl.50686

600 Wang S, Zhang Y, Ju W, et al (2020) Recent global decline of CO_2 fertilization effects
601 on vegetation photosynthesis. Science 370:1295–1300.
602 https://doi.org/10.1126/science.abb7772

603 Wu Y, Liu S, Abdul-Aziz O (2012) Hydrological Effects of the Increased CO2 and
604 Climate Change in the Upper Mississippi River Basin Using a Modified SWAT.
605 Clim Change 110:977–1003. https://doi.org/10.1007/s10584-011-0087-8

606 Xiao M, Yu Z, Kong D, et al (2020) Stomatal response to decreased relative humidity
607 constrains the acceleration of terrestrial evapotranspiration. Environ Res Lett
608 15:094066. https://doi.org/10.1088/1748-9326/ab9967

609 Yang Y, Roderick ML, Zhang S, et al (2019) Hydrologic implications of vegetation
610 response to elevated CO_2 in climate projections. Nat Clim Change 9:44–48.
611 https://doi.org/10.1038/s41558-018-0361-0

612

613